A MODE III MOVING CRACK BETWEEN A FUNCTIONALLY GRADED COATING AND A HOMOGENEOUS SUBSTRATE

Bao-Lin Wang and Jie-Cai Han

A MODE III MOVING CRACK BETWEEN A FUNCTIONALLY GRADED COATING AND A HOMOGENEOUS SUBSTRATE

BAO-LIN WANG AND JIE-CAI HAN

This paper considers an anti-plane moving crack between a functionally graded coating and a homogeneous substrate. The shear modulus and the mass density of the FGM coating are considered for a class of functional forms for which the equilibrium equation has an analytical solution. The problem is solved by means of singular integral equation technique. Results are plotted to show the effect of material nonhomogeneity and crack moving velocity on the crack tip field. The angular variation of the near-tip stress field is of particular interest, and the crack bifurcation behaviour is also discussed. It is shown that choice of an appropriate fracture criterion is essential for studying the stability of a moving crack in FGMs. Different fracture criteria could give opposite predictions for crack stability. It seems that the maximum cleavage stress near the crack tips is a reasonable failure criterion for a moving crack in FGMs.

1. Introduction

In functionally graded materials, the compositions and microstructures vary continuously in the thickness direction and the mismatch of material properties at the coating/substrate interface is eliminated. The problem of cracks in functionally graded materials has been studied extensively. In particular, some authors have studied dynamic fracture problems of FGMs. Marur and Tippur [1998] computed the magnitude and phase of complex stress intensity factors in FGMs for static and dynamic loading. Rousseau and Tippur [2001] studied the effect of different elastic gradient profiles on the fracture behavior of dynamically loaded functionally graded materials with cracks parallel to the elastic gradient. They used finite-element analyses of FGM and homogeneous beams to examine crack tip responses to low velocity and symmetric impact loading on the uncracked edge of the beams. Wu et al. [2002] proposed an extended dynamic J integral for functional graded materials. Zhang et al. [2003] used a boundary integral equation method to investigate the dynamic response of FGM crack problems. Chen et al. [2003] investigated the dynamic fracture of a crack in a functionally graded piezoelectric interface. Guo et al. [2005] considered the dynamic response of an edge crack in a functionally

graded orthotropic strip. Zhou et al. [2004] investigated the dynamic behavior of
a finite crack in functionally graded materials using the Schmidt method. The dy-
namic propagations of anti-plane shear cracks in functionally graded piezoelectric
strips have been investigated by Kwon [2004] and Shin et al. [2004]. Recently,
Sladek et al. [2005] used a meshless local boundary integral equation method for
dynamic anti-plane shear crack problems in functionally graded materials.

   All these papers considered the time dependence of the crack tip field in FGMs.
Solutions to problems of moving cracks in FGMs are important since they can
assist in the understanding of how FGMs can best be constructed to arrest running
cracks. Some earlier investigations [Jin et al. 2003; Bi et al. 2003; Jin and Zhong
2002; Li and Weng 2002; Ma et al. 2005] have considered moving cracks in FGMs
with exponentially distributed material properties.

   In this paper, we study a crack moving at the interface between an FGM layer and
a homogeneous substrate. The properties of the FGM are considered for a class of
continuous functions of the coordinate perpendicular to the crack plane. The Yoffe
model [1951] of a running crack is adopted. The crack is assumed to propagate at a
constant velocity. The results show that crack growth behavior is strongly affected
by the material nonhomogeneity and the crack moving velocity. Different fracture
criteria may lead to different, indeed opposite, crack growth predictions. This
suggests that the selection of a fracture criterion is essential for moving cracks in
FGMs. Based on the maximum cleavage stress criterion, the dependence of crack
bifurcation angle and the critical crack speed (at which bifurcation occurs) on the
stress intensity factor are found to be identical for functionally graded materials
and homogeneous materials. Stress intensity factors, however, have a strong de-
pendence on material nonhomogeneity and crack moving velocity.

2. Formulation of the crack problem

From the viewpoint of applications, anti-plane crack problems often provide a
useful analog to the more interesting in-plane fracture problems. Therefore, we
investigate an anti-plane crack problem in an FGM/substrate structure. The prop-
erties of the FGM vary along the y-axis, as shown in Figure 1. There is a plane
crack of length $2a$ lying at the interface between the FGM and the substrate. The
crack advances with a constant length in the material having shear modulus $\mu(Y)$
and mass density $\rho(Y)$. Crack motion is maintained at a constant velocity V by
the uniform anti-plane shear stress $-\tau_0(x)$ applied to the crack faces.

   We call XY the fixed coordinate system and xy the coordinates attached to the
moving crack. Under anti-plane deformation, the constitutive equations are

$$\tau_{xz} = \mu(Y)\frac{\partial w}{\partial X}, \qquad \tau_{yz} = \mu(Y)\frac{\partial w}{\partial Y}, \tag{1}$$
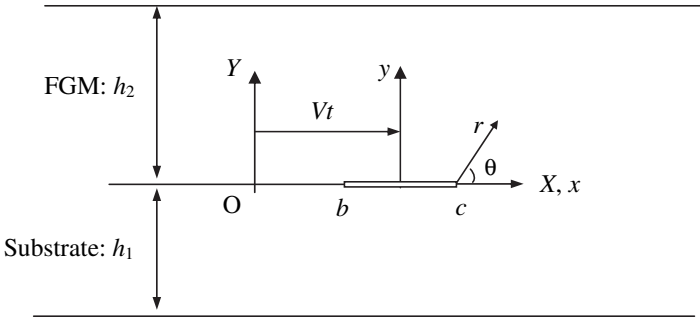
Figure 1. Geometry of the crack problem.

where $\mu(Y)$ is the shear modulus, which is a constant for $y < 0$. From the equilibrium equation

$$\frac{\partial \tau_{xz}}{\partial X} + \frac{\partial \tau_{yz}}{\partial Y} = \rho \frac{\partial^2 w}{\partial t^2}$$

and the constitutive equations, we obtain

$$\mu(Y)\left(\frac{\partial^2 w}{\partial X^2} + \frac{\partial^2 w}{\partial Y^2}\right) + \frac{d\mu(Y)}{dY}\frac{\partial w}{\partial Y} = \rho(Y)\frac{\partial^2 w}{\partial t^2}.$$

To simplify this equation, we apply the coordinate change $x = X - Vt$, obtaining

$$\mu(y)\left(\frac{\partial^2 w}{\partial x^2} + \frac{\partial^2 w}{\partial y^2}\right) + \frac{d\mu(y)}{dy}\frac{\partial w}{\partial y} - V^2\rho(y)\frac{\partial^2 w}{\partial x^2} = 0. \tag{2}$$

Let the solution of (2) be given by

$$w(x, y) = \frac{1}{2\pi}\int_{-\infty}^{\infty} F(y, s)e^{-isx}\, ds \tag{3}$$

(see [Erdogan and Ozturk 1992]), where the function F is to be determined. It follows from (2) and (3) that

$$\frac{d^2 F}{dy^2} + p(y)\frac{dF}{dy} - \left(1 - \frac{V^2\rho(y)}{\mu(y)}\right)s^2 F = 0, \tag{4}$$

where

$$p(y) = \frac{\mu'(y)}{\mu(y)}.$$

To overcome the complexity of mathematics involved, we will focus in this study on a special class of FGMs in which the properties vary proportionally, that is,

$$\mu(y) = \mu_0 f(y) \quad \text{and} \quad \rho(y) = \rho_0 f(y) \tag{5}$$

for some function $f(y)$, where μ_0 and ρ_0 are material properties of the homogeneous substrate. From equations (4) and (5), we obtain

$$\frac{d^2 F}{dy^2} + p(y)\frac{dF}{dy} - \omega^2 s^2 F = 0, \tag{6}$$

where

$$\omega = \sqrt{1 - (V/c)^2} \quad \text{with} \quad c = \sqrt{\mu_0/\rho_0}$$

is the lowest bulk wave speed for plane wave propagation along the x direction. Introduce the function

$$H(y, s) = F(y, s)f(y)^{1/2}. \tag{7}$$

Then Equation (6) becomes

$$\frac{d^2 H}{dy^2} - \frac{1}{4}\left(p^2 + 2\frac{dp}{dy} + 4s^2\omega^2\right)H = 0. \tag{8}$$

We will now look for a particular class of functions for which this equation has an analytical solution. The simplest class of such functions is obtained by assuming that

$$p^2 + 2\frac{dp}{dy} = 4\ell_0,$$

where ℓ_0 is a constant. We consider three classes of functions satisfying this equation (see [Erdogan and Ozturk 1992; Wang et al. 2003]):

(a) With $\ell_0 > 0$ and $\beta = \sqrt{\ell_0}$:

$$
\begin{aligned}
p(y) &= \mp 2\beta, & f(y) &= \exp(\mp 2\beta y), \\
p(y) &= 2\beta \coth(\beta y + 0.8814), & f(y) &= \sinh^2(\beta y + 0.8814), \\
p(y) &= 2\beta \tanh(\beta y), & f(y) &= \cosh^2(\beta y).
\end{aligned}
\tag{9}
$$

(b) With $\ell_0 < 0$ and $\beta = \sqrt{-\ell_0}$:

$$p(y) = -2\beta \tan(\beta y), \qquad f(y) = \cos^2(\beta y). \tag{10}$$

(c) With $\ell_0 = 0$ and β arbitrary:

$$
\begin{aligned}
p(y) &= 2\beta/(\beta y + 1), & f(y) &= (\beta y + 1)^2, \\
p(y) &= 0, & f(y) &= 1.
\end{aligned}
\tag{11}
$$

The material properties are continuous at the interface between the coating and the substrate if the coating property gradient is described by any of these equations. The case $p = 0$, $f = 1$ describes a homogeneous coating.

3. The solutions

For the choices of $p(y)$ and $f(y)$ just listed, Equation (8) can be solved in analytic form:

$$H = A(s) \exp(|s|\gamma y) + B(s) \exp(-|s|\gamma y), \qquad \gamma = \sqrt{\omega^2 + \ell_0/s^2}, \qquad (12)$$

where A and B are arbitrary constants. It follows from (12), (7) and (3) that

$$w(x, y) = \frac{1}{2\pi} \int_{-\infty}^{\infty} \left(f_{1a}(y)A_1(s) + f_{1b}(y)B_1(s) \right) e^{-isx} \, ds, \quad -h_1 < y < 0,$$

$$w(x, y) = \frac{1}{2\pi} \int_{-\infty}^{\infty} \left(f_{2a}(y)A_2(s) + f_{2b}(y)B_2(s) \right) e^{-isx} \, ds, \qquad h_2 > y > 0,$$

$$(13)$$

where $A_1(s)$, $B_1(s)$, $A_2(s)$ and $B_2(s)$ are unknown functions and

$$\begin{aligned}
f_{1a}(y) &= e^{|s|\omega y}, & f_{1b}(y) &= e^{-|s|\omega y}, \\
f_{2a}(y) &= f(y)^{-1/2} e^{|s|\gamma y}, & f_{2b}(y) &= f(y)^{-1/2} e^{-|s|\gamma y}.
\end{aligned} \qquad (14)$$

In formulating those boundary conditions, the crack problem has been treated using the superposition technique; that is, the problem without any cracks has been solved and the equal and opposite values of the stresses have been used as the applied loads on the crack surfaces. Therefore, the boundary and continuity conditions are as follows (see Figure 1):

$$\tau_{yz}(x, -h_1) = 0 = \tau_{yz}(x, h_2) \quad \text{for} x \in (-\infty, \infty), \qquad (15)$$

$$\tau_{yz}(x, +0) = \tau_{yz}(x, -0) \quad \text{for} x \in (-\infty, \infty), \qquad (16)$$

$$w(x, +0) = w(x, -0) \quad \text{for} x \notin (b, c), \qquad (17)$$

$$\tau_{yz}(x, +0) = \tau_{yz}(x, -0) = \tau_0(x) \quad \text{for} x \in (b, c). \qquad (18)$$

Those conditions can be used to determine the unknown constants $A_1(s)$, $B_1(s)$, $A_2(s)$ and $B_2(s)$.

3.1. *The singular integral equation.*
The three homogeneous boundary conditions shown in Equations (15) and (16) can be used to eliminate three of the four unknown functions. The mixed boundary conditions (17)–(18) then give a system of dual integral equations to determine the remaining one. By defining a new unknown function

$$g(x) = \frac{\partial w(x, +0) - \partial w(x, -0)}{\partial x}, \qquad (19)$$

the problem can be reduced to an integral equation in g; then it is seen that (17) is equivalent to

$$g(x) = 0 \text{ for } x \notin (b, c) \qquad \int_b^c g(x)\,dx = 0,$$

and (18) gives the desired integral equation.

By substituting the values from Equations (13) via Hooke's law into the boundary conditions (15) and continuity conditions (16), and by using Equation (19), we can determine $A_1(s)$, $B_1(s)$, $A_2(s)$ and $B_2(s)$ in terms of the Fourier transforms of g. Noting that g is zero for $x \notin (b, c)$, the expressions found for $A_1(s)$, $B_1(s)$, $A_2(s)$ and $B_2(s)$ are

$$A_1(s) = \frac{1}{\Delta(s)}\left(f_{2a}'(0) - f_{2b}'(0)\frac{f_{2a}'(h_2)}{f_{2b}'(h_2)} \right)\frac{i}{s}\int_b^c g(t)e^{ist}dt,$$

$$B_1(s) = \exp(-2|s|\omega h_1)A_1(s),$$

$$A_2(s) = \frac{1}{\Delta(s)}\left(f_{1a}'(0) - f_{1b}'(0)\frac{f_{1a}'(-h_1)}{f_{1b}'(-h_1)} \right)\frac{i}{s}\int_b^c g(t)e^{ist}dt,$$

$$B_2(s) = -\frac{f_a'(h_2)}{f_b'(h_2)}A_2(s),$$

where

$$f_a'(y) = \partial f_a(y)/\partial y, \qquad f_b'(y) = \partial f_b(y)/\partial y,$$

and

$$\Delta(s) = \left(1 - \frac{f_{2a}'(h_2)}{f_{2b}'(h_2)} \right)\left(f_{1a}'(0) - f_{1b}'(0)\frac{f_{1a}'(-h_1)}{f_{1b}'(-h_1)} \right)$$
$$- \left(1 - \frac{f_{1a}'(-h_1)}{f_{1b}'(-h_1)} \right)\left(f_{2a}'(0) - f_{2b}'(0)\frac{f_{2a}'(h_2)}{f_{2b}'(h_2)} \right).$$

Substituting Equations (1) and (13) into the remaining boundary condition (18), we obtain:

$$\frac{1}{\pi}\int_b^c g(t)K(x, t)\,dt = \tau_0(x)/\mu_0, \tag{20}$$

where

$$K(x, t) = \frac{i}{2}\int_{-\infty}^{\infty} k(s)e^{is(t-x)}ds, \tag{21}$$

$$k(s) = \frac{1}{s\,\Delta(s)}\left(f_{1a}'(0) - f_{1b}'(0)\frac{f_{1a}'(-h_1)}{f_{1b}'(-h_1)} \right)\left(f_{2a}'(0) - f_{2b}'(0)\frac{f_{2a}'(h_2)}{f_{2b}'(h_2)} \right). \tag{22}$$

Therefore, the integral kernel k can be obtained by inserting the property distributions (9)–(11) into Equations (14) and then into (22).

To determine the singular behavior of (20) we must examine the behavior of the kernel k. For this, it is sufficient to determine and separate those leading terms in the asymptotic expansion of k as $|s| \to \infty$ that would lead to unbounded integrals. From the expression of k in (22) it can be shown that in the asymptotic expansions for $|s| \to \infty$ the only terms that would give unbounded integrals are

$$k(\pm\infty) = -\operatorname{sgn}(s)\tfrac{1}{2}\omega.$$

By adding and substituting this asymptotic value to and from k in (21), and by evaluating the integrals involving the leading terms, we obtain

$$K(x,t) = \tfrac{1}{2}\omega\,\frac{1}{t-x} + \frac{i}{2}\int_{-\infty}^{\infty}\Lambda(s)e^{is(t-x)}\,ds,$$

where

$$\Lambda(s) = k(s) + \tfrac{1}{2}\operatorname{sgn}(s)\omega.$$

Thus, Equation (20) becomes

$$\frac{\omega}{2\pi}\int_{b}^{c}\frac{1}{t-x}g(t)\,dt + \frac{1}{\pi}\int_{b}^{c}K_1(x,t)g(t)\,dt = \frac{\tau_0(x)}{\mu_0}, \qquad (23)$$

where

$$K_1(x,t) = \frac{i}{2}\int_{-\infty}^{\infty}\Lambda(s)e^{is(t-x)}ds = -\int_{0}^{\infty}\Lambda(s)\sin\big(s(t-x)\big)\,ds$$

is a known bounded function.

3.2. *The crack tip field.* Equation (23) contains a Cauchy-type kernel. Consequently, the crack tip behavior can be characterized by a standard square-root singularity. The solution of the singular integral equation (23) has the form

$$g(x) = \frac{G(x)}{\sqrt{(x-b)(c-x)}}, \qquad (24)$$

where G is a bounded function. After normalizing the interval (b,c), equation (23) can be solved numerically by using a Gaussian quadrature formula. The mode III stress intensity factor at, for example, at the crack tip $x = b$ is defined by

$$k_3(b) = \lim_{x \to b-0}\sqrt{2(x-b)}\,\tau_{yz}(x,0).$$

Observing that Equation (23) gives the stress component $\tau_{yz}(x,0)$ on the plane of the crack for $x \in (b,c)$ as well as $x \notin (b,c)$, and substituting from (24) into (23), a simple asymptotic analysis shows that

$$k_3(b) = \frac{\mu_0}{2}\omega\frac{G(b)}{\sqrt{a}}, \qquad k_3(c) = -\frac{\mu_0}{2}\omega\frac{G(c)}{\sqrt{a}}.$$

Of practical interest is the stress status near the crack tip. From the above results we can obtain the asymptotic fields near the moving crack tips in terms of the stress intensity factor in the moving coordinate system. The results at the right crack tip are

$$\tau_{yz} = \frac{k_3(c)}{\sqrt{2\pi\hat{r}}} \cos\frac{\hat{\theta}}{2}, \qquad \tau_{xz} = -\frac{k_3(c)}{\omega\sqrt{2\pi\hat{r}}} \sin\frac{\hat{\theta}}{2}, \qquad (25)$$

where

$$\hat{r} = \sqrt{(x-a)^2 + (\omega y)^2}, \qquad \hat{\theta} = \tan^{-1}\frac{\omega y}{x-a}. \qquad (26)$$

4. Infinite functionally graded medium

The foregoing analysis can be easily extended to the case of an infinite functionally graded medium ($h_1 \to \infty$ and $h_2 \to \infty$). Suppose by using superposition technique, the solution has been reduced to a perturbation problem where the only applied loads are the anti-plane shear stresses on the crack surfaces. To satisfy the regularity conditions at infinity, the constants B_1 and A_2 in Equations (13) must equal zero. Following a similar analysis procedure in Section 3, we obtain the remaining unknown constants B_2 and A_1 as

$$A_1(s) = \frac{f'_{2b}(0)}{f'_{1a}(0) - f'_{2b}(0)} \frac{i}{s} \int_b^c g(t)e^{ist}dt,$$

$$B_2(s) = \frac{f'_{1a}(0)}{f'_{1a}(0) - f'_{2b}(0)} \frac{i}{s} \int_b^c g(t)e^{ist}dt.$$

The integral equation (20) remains unchanged, provided that the integral kernel $k(s)$ in (21) be replaced by

$$k(s) = \frac{f'_{1a}(0)f'_{2b}(0)}{s[f'_{1a}(0) - f'_{2b}(0]}.$$

The rest of the analysis and the equation system are the same as those in the previous section.

5. Results and discussion

We have considered an infinite medium ($h_1 \to \infty$, $h_2 \to \infty$) with proportional material properties $f(y)$ and $p(y)$ varying according to one of several functions, namely, $f(y) = \exp(\beta y)$, $f(y) = \sinh^2(\beta y + 0.8814)$, and $f(y) = \exp(-\beta y)$. The latter represents a soft coating (the stiffness of the coating is less than that of the substrate). The values of the stress intensity factors for a single crack are given in Figure 2, where $a = (c-b)/2$ is the half-crack length. As expected, the value of k_3 for a homogeneous medium ($\beta = 0$) is 1 for any crack velocity. For
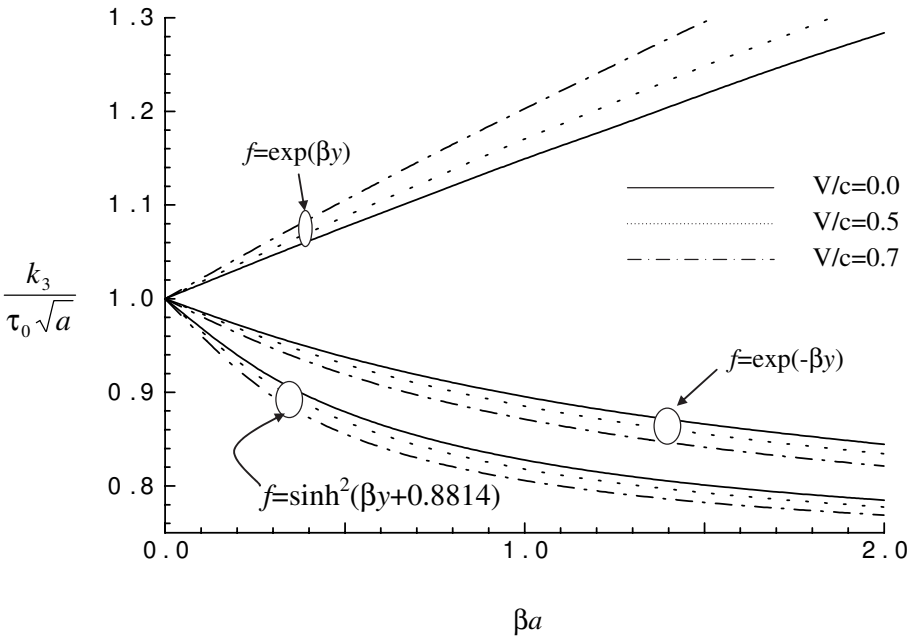
Figure 2. Stress intensity factors for a crack at different velocities.

the property distribution $f(y) = \exp(\beta y)$, the values of the stress intensity factor k_3 increase with the material nonhomogeneity β and the crack moving velocity V. Oppositely, for the property distributions $f(y) = \exp(-\beta y)$ and $f(y) = \sinh^2(\beta y + 0.8814)$, the values of k_3 decrease with the material nonhomogeneity and the crack moving velocity. The results indicate further that for a nonhomogeneous material with property distributions $f(y) = \exp(-\beta y)$ and $f(y) = \sinh^2(\beta y + 0.8814)$ the stress intensity factor k_3 is smaller than the corresponding value for a homogeneous material.

The fact that the values of k_3 can increase or decrease with crack moving velocities suggests that, if the stress intensity factor criterion is used to predict the unstable fracture initiation, then the critical applied loads can increase or decrease with crack velocities, depending on the type of the material nonhomogeneity (gradient). For example, unstable fracture is more likely to take place, for a lower crack moving velocity, for material gradient $f(y) = \sinh^2(\beta y + 0.8814)$, and for a higher crack moving velocity, for material gradient $f(y) = \exp(\beta y)$.

For a quick assessment of a possible unstable crack growth initiation, it is generally sufficient to examine the amplitude and the direction of the maximum cleavage stress $\tau_{\theta z}(r, \theta)$ at the crack tips. The cleavage stress $\tau_{\theta z}(r, \theta)$ can be expressed as

$$\tau_{\theta z}(r, \theta) = \tau_{yz} \cos \theta - \tau_{xz} \sin \theta, \tag{27}$$

where (r, θ) are the polar coordinates at the crack tip and θ is measured from
the positive x-axis (see Figure 1). Figure 3 gives the variation of cleavage shear
stress $\tau_{\theta z}(r, \theta)$ with the angle for different crack velocities. It is seen that the
stresses depend significantly on the crack velocities. Unlike the static solution, the
maximum value of $\tau_{\theta z}(r, \theta)$ does not always occur along the axis coincident with
the crack ($\theta = 0$). For small velocities, the shear stress decreases monotonously
with the angle. As the velocity increases, $\tau_{\theta z}(r, \theta)$ in each curve attains a maximum
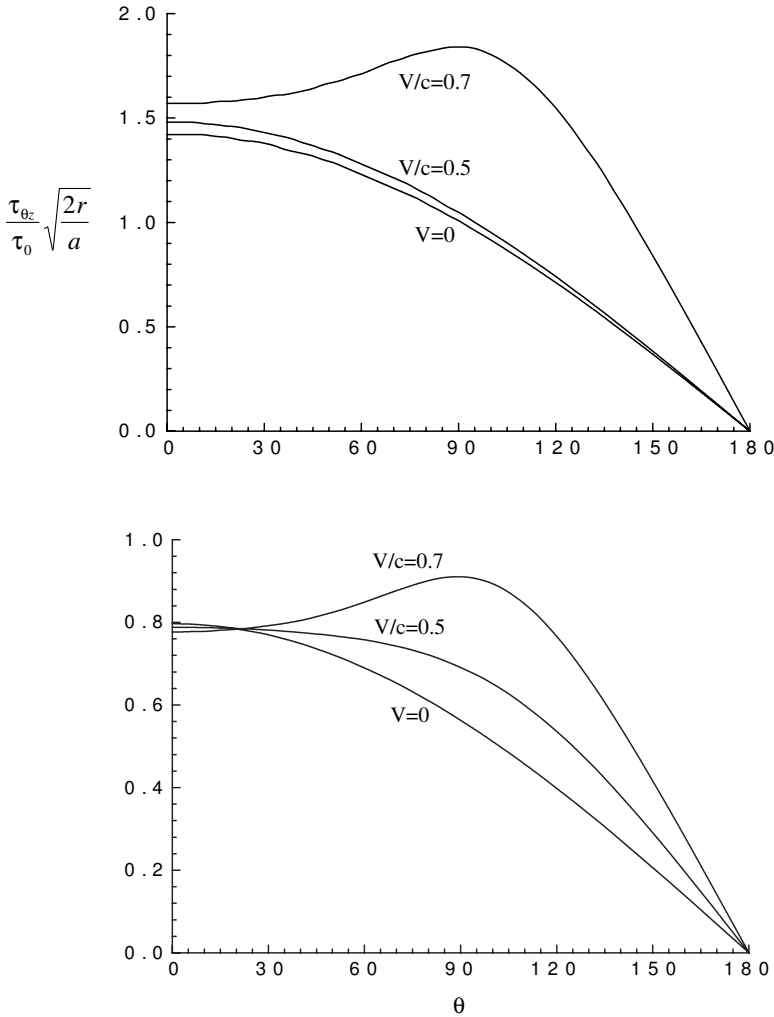

Figure 3. Angular distribution of stress $\tau_{\theta z}$ with polar angle for a
crack moving at different velocities. Top: $f = \exp(\beta y)$, $\beta a = 3$.
Bottom: $f = \sinh^2(\beta y + 0.8814)$, $\beta a = 1.5$.

value at an angle different from $\theta = 0$. This suggests that crack bifurcation may occur at a sufficient higher crack moving velocity.

Further consideration of the results in Figure 3 shows that the peak values of the cleavage stress $\tau_{\theta z}(r, \theta)$ increase with the crack moving velocity, both for the gradient $f(y) = \exp(\beta y)$ and for the gradient $f(y) = \sinh^2(\beta y + 0.8814)$. Hence, it is more reasonable to use the maximum cleavage stress $\tau_{\theta z}(r, \theta)$ as a fracture criterion, since it can predict that the fracture is more likely to take place for a higher crack moving velocity, no matter what kind of material nonhomogeneity the medium has.

As mentioned above, the crack may bifurcate at a sufficient high moving velocity. Referring to Figure 3, the bifurcation angle θ_c and the critical crack speed at which bifurcation initiation can be found from:

$$\frac{\partial \tau_{\theta z}(r, \theta_c)}{\partial \theta_c} = 0, \qquad \frac{\partial^2 \tau_{\theta z}(r, \theta_c)}{\partial \theta_c^2} < 0. \tag{28}$$

From Equations (25), (26), (27) and (28) we see that the value of θ_c is only a function of crack moving velocities and does not depend on the material gradient. Therefore, the bifurcation angle θ_c and the critical crack speed at which bifurcation occurs are the same as for an ordinary homogeneous isotropic solid.

6. Conclusions

The fracture problem for a functionally graded material under anti-plane shear loads is investigated for a class of property distributions. The paper aims at determining the crack tip stress field, evaluating simultaneously the effects of the crack velocity and material varying properties. Also discussed are the stability of crack growth, crack bifurcation and failure criteria to be adopted. The following conclusions can be drawn:

- Unlike the case of a a homogeneous coating, crack motion affects the stress intensity factors for an FGM coating.

- Stress intensity factors depend on the crack velocity as well as material nonhomogeneity. They can increase or decrease with material nonhomogeneities and crack velocities, depending on the type of the material property distribution.

- For a stationary crack, the angular distribution of the stress field near the crack tips is the same as for a homogeneous material. But for a moving crack the singular stress field near the crack tips is altered considerably by crack velocity.

- It is more convenient to use the maximum cleavage stress $\tau_{\theta z}(r, \theta)$ as a fracture criterion for a moving crack in FGMs, since it can explain the fact that the

fracture is more likely to take place for a higher moving velocity, for any of the kinds of material nonhomogeneity (gradients) considered in this paper. Oppositely, if the stress intensity factor criterion is used, the crack growth could be enhanced or retarded by crack moving velocity, depending on the material nonhomogeneity.

Acknowledgements

References

[Bi et al. 2003] X. S. Bi, J. Cheng, and X. L. Chen, "Moving crack for functionally grated material in an infinite length strip under antiplane shear", *Theor. Appl. Fract. Mech.* **39**:1 (2003), 89–97.

[Chen et al. 2003] J. Chen, Z. Liu, and Z. Zou, "Dynamic response of a crack in a functionally graded interface of two dissimilar piezoelectric half-planes", *Arch. Appl. Mech.* **72**:9 (2003), 686–696.

[Erdogan and Ozturk 1992] F. Erdogan and M. Ozturk, "Diffusion problems in bonded nonhomogeneous materials with an interface cut", *Int. J. Eng. Sci.* **30**:10 (1992), 1507–1523.

[Guo et al. 2005] L. C. Guo, L. Z. Wu, and T. Zeng, "The dynamic response of an edge crack in a functionally graded orthotropic strip", *Mech. Res. Commun.* **32**:4 (2005), 385–400.

[Jin and Zhong 2002] B. Jin and Z. Zhong, "A moving mode-III crack in functionally graded piezoelectric material: permeable problem", *Mech. Res. Commun.* **29**:4 (2002), 217–224.

[Jin et al. 2003] B. Jin, A. K. Soh, and Z. Zhong, "Propagation of an anti-plane moving crack in a functionally graded piezoelectric strip", *Arch. Appl. Mech.* **73**:3–4 (2003), 252–260.

[Kwon 2004] S. M. Kwon, "On the dynamic propagation of an anti-plane shear crack in a functionally graded piezoelectric strip", *Acta Mech.* **167**:1–2 (2004), 73–89.

[Li and Weng 2002] C. Y. Li and G. J. Weng, "Yoffe-type moving crack in a functionally graded piezoelectric material", *P. Roy. Soc. Lond. A Mat.* **458**:2018 (2002), 381–399.

[Ma et al. 2005] L. Ma, L. Z. Wu, L. C. Guo, and Z. G. Zhou, "On the moving Griffith crack in a non-homogeneous orthotropic medium", *Eur. J. Mech. A: Solids* **24**:3 (2005), 393–405.

[Marur and Tippur 1998] P. R. Marur and H. V. Tippur, "Evaluation of mechanical properties of functionally graded materials", *J. Test. Eval.* **26**:6 (1998), 539–545.

[Rousseau and Tippur 2001] C.-E. Rousseau and H. V. Tippur, "Influence of elastic gradient profiles on dynamically loaded functionally graded materials: cracks along the gradient", *Int. J. Solids Struct.* **38**:44–45 (2001), 7839–7856.

[Shin et al. 2004] J. W. Shin, T. U. Kim, and S. C. Kim, "Dynamic characteristics of an eccentric crack in a functionally graded piezoelectric ceramic strip", *Korean Soc. Mech. Eng. Int. J.* **18**:9 (2004), 1582–1589.

[Sladek et al. 2005] J. Sladek, V. Sladek, and C. Z. Zhang, "A meshless local boundary integral equation method for dynamic anti-plane shear crack problem in functionally graded materials", *Eng. Anal. Bound. Elem.* **29**:4 (2005), 334–342.

[Wang et al. 2003] B. L. Wang, Y. W. Mai, and Y. G. Sun, "Anti-plane fracture of a functionally graded material strip", *Eur. J. Mech. A: Solids* **22**:3 (2003), 357–368.

[Wu et al. 2002] C. Wu, P. He, and Z. Li, "Extension of *J* integral to dynamic fracture of functional graded material and numerical analysis", *Comput. Struct.* **80**:5–6 (2002), 411–416.

[Yoffe 1951] E. H. Yoffe, "The moving Griffith crack", *Philos. Mag.* **42**:7 (1951), 739–750.

[Zhang et al. 2003] C. Zhang, A. Savaidis, G. Savaidis, and H. Zhu, "Transient dynamic analysis of a cracked functionally graded material by a BIEM.", *Comput. Mater. Sci.* **26** (2003), 167–174.

[Zhou et al. 2004] Z. G. Zhou, B. Wang, and Y. G. Sun, "Investigation of the dynamic behavior of a finite crack in the functionally graded materials by use of the Schmidt method", *Wave Motion* **39**:3 (2004), 213–225.

BAO-LIN WANG: wangbl2001@hotmail.com
Centre for Advanced Materials Technology (CAMT), School of Aerospace, Mechanical and Mechatronic Engineering, The University of Sydney, Sydney, NSW 2006, Australia

JIE-CAI HAN: hanjc@hit.edu.cn
Center for Composite Materials, Harbin Institute of Technology, Harbin 150001, P.R. China